Magnesium Technology 2013
Edited by: Norbert Hort, Suveen N. Mathaudhu, Neale R. Neelameggham, and Martyn Alderman
TMS (The Minerals, Metals & Materials Society), 2013

MICROSTRUCTURE AND TEXTURE EVOLUTION IN A MAGNESIUM ALLOY DURING EXTRUSION AT VARIOUS EXTRUSION SPEEDS

Q. Ma[1], S.J. Horstemeyer[1], B. Li[1], Z. McClelland[1], P.T. Wang[1], M.F. Horstemeyer[1,2]

[1]. Center for Advanced Vehicular Systems, Mississippi State University, Starkville, MS 39759, USA
[2]. Department of Mechanical Engineering, Mississippi State University, Starkville, MS 39762, USA

Keywords: Magnesium; Texture; Twinning; Recrystallization; EBSD.

Abstract

An AM30 magnesium alloy was extruded by using a lab-scale flat die at ~450 °C and various ram speeds: 5 mm/min, 10 mm/min, 20 mm/min, 30 mm/min, and 50 mm/min, respectively. Microstructure and texture in the representative locations inside the die and the extrudate of the AM30 at different ram speeds were examined by electron backscatter diffraction (EBSD). Significant dynamic recrystallization (DRX) occurred inside the die, whereas static recrystallization (SRX) took over in the extrudate outside the die. Profuse $\{10\bar{1}2\}\langle 10\bar{1}\bar{1}\rangle$ extension twinning activated during extrusion at low ram speed of 10 mm/min, but twinning was hardly observed at high ram speed of 50 mm/min. DRX and SRX led to different microstructure evolution at different extrusion speeds. Possible mechanisms that govern the DRX and the SRX were analyzed.

Introduction

Magnesium (Mg) alloys are potential lightweight materials for automotive and aerospace industry. But the low ductility of Mg and its alloys at ambient temperature hinders their applications. Wrought Mg alloys are usually subjected to deformation at high temperature, e.g. extrusion at temperatures typical of 350-450 °C [1-3]. Extrusion is an important thermomechanical processing for Mg alloys in industry. Though extensive studies have been performed on simple compression, tension, rolling and extrusion of Mg alloys at elevated temperatures, there are limited studies focused on how microstructure and texture evolve during extrusion inside the die [3]. In extrusion, deformation and dynamic recrystallization (DRX) inside the die, and the subsequent static recrystallization (SRX) outside the die dominate the final microstructure, texture and property of the product. Since the stress state in extrusion differs from uniaxial compression, tension, and rolling, the deformation, DRX and SRX mechanisms during extrusion should exhibit different characteristics. Therefore, understanding the mechanisms of deformation and recrystallization of Mg alloy during extrusion is of significance for process optimization.

It is well known that twinning, basal slip, prismatic slip, <c+a> slip and DRX are strongly affected by temperature and strain rate [4-5]. Conceivably, DRX and SRX will be influenced by extrusion temperature and extrusion speed as well. However, at typical extrusion temperature of around 450 °C, how the extrusion ram speed change influences the microstructure and texture of the extrudate of Mg alloy is still not fully understood.

The aim of this work is to investigate the effect of extrusion speed on the microstructure and texture evolution of a commercial Mg alloy during a lab-scale flat-die extrusion at 450 °C.

Experimental

A commercial extruded Mg alloy billet AM30 (Al 2.54%, Mn 0.40%, balance Mg, wt%) with a diameter of 178 mm from Timminco Metals Corporation was selected as the experimental material. The cylindrical lab-scale extrusion billet was cut from the as-extruded AM30 billet with the axis parallel to the extrusion direction (ED). The lab-scale billet had a diameter of 31.8 mm and a height of 25.4 mm. An in-house lab-scale flat die was used in this study. The extrudate has a diameter of 6.35 mm. The extrusion ratio is 25.1. The flat die was fixed in a furnace chamber that held the sample stage of the INSTRON 8850 machine. A high temperature graphite paste GPL-420 was used as lubricant during extrusion. The lab-scale extrusion billet was heated up to 450 °C inside the die and soaked for 30 minutes. Then the billet was indirectly extruded at different ram speeds as: 5 mm/min, 10 mm/min, 20 mm/min, 30 mm/min, and 50 mm/min, respectively. After extrusion, the AM30 extrusion butt inside the flat die and the extrudate outside the die were cut and cold mounted to study the microstructure. The cold mounted samples were polished using series SiC papers down to a grit number of 4000. Then the AM30 samples were polished using alumina (down to 0.05 μm) suspended in ethylene glycol. The polished samples were etched using a solution of HNO_3 and acetic acid [5]. The etched samples were then examined by electron backscatter diffraction (EBSD) scan in the different representative positions inside the die or in the extrudate outside the die. Some samples and the extrusion butts were also examined by optical microscope (OM) to characterize the microstructure change of the AM30. Figure 1 presents the lab-scale flat die and the extrusion fixture in this study.

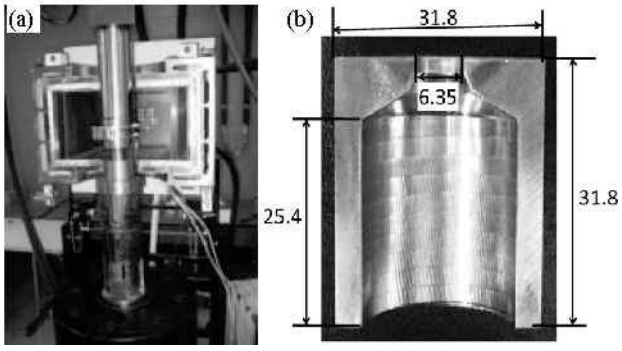

Figure 1: Lab-scale extrusion fixture inside the furnace chamber on the INSTRON 8850 machine (a), and a magnified picture of the flat die section (b).

Results

After extrusion, the extrusion butt of the AM30 inside the die was cut along ED with the cut section comprising the die axis. Figure 2 presents typical optical microscope (OM) pictures at different representative positions termed as Top, Middle, and Exit positions inside the die of AM30. The microstructure in the extrudate of AM30 exit far outside the die is defined as the Extrudate position.

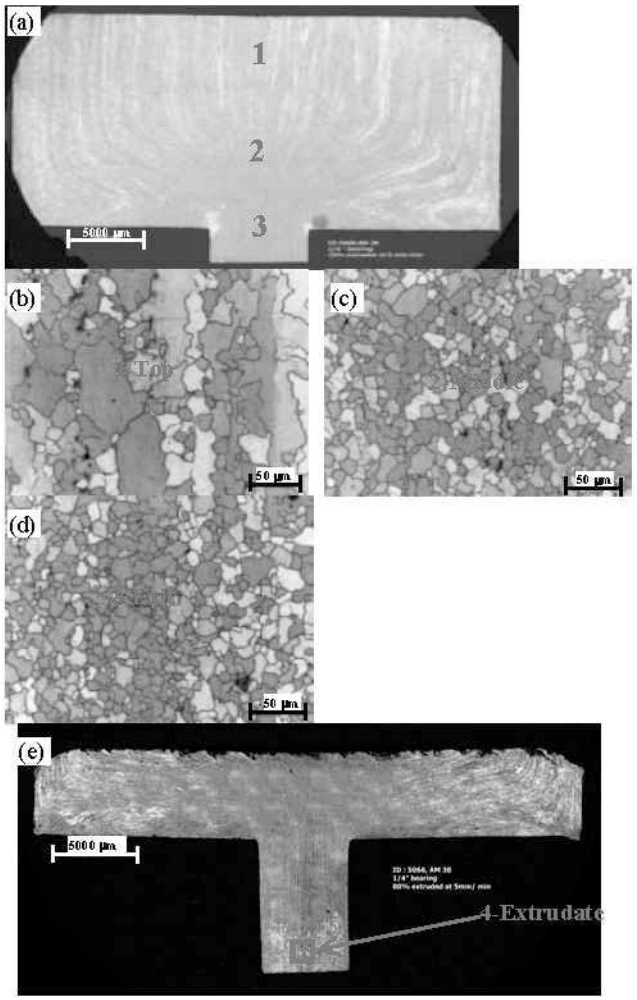

Figure 2: Optical microscope microstructure of the AM30 during extrusion at different representitive positions inside the die and the extrudate extruded at 450 °C and ram speed of 5 mm/min. (a) representitive positions inside the flat die.1-Top, 2-Middle, 3-Exit; (b) Top microstructure; (c) Middle microstructure; (d) Exit microstructure; and (e) the Extrudate position and the extrsuion butt. Extrusion flow lines and different microstructures can be seen in (a) and (b)-(e), respectively.

As shown in Figure 2, microstructure dynamically changes during extrusion. The big grain zone appears in the extrudate due to grain growth after extrusion by the meta-dynamic recrystallization or SRX. Microstructure and texture scanned by EBSD in different representative positions of the AM30 extruded at ram speed of 10, 20, 30, and 50 mm/min are presented in Figures 3-6.

At ram speed of 10 mm/min, both microstructure and texture significantly change during extrusion (Figure 3). The texture in the Middle and the Exit position differ, but texture in the Exit and the Extrudate position are similar where $\langle 10\bar{1}0\rangle$ and $\langle 2\bar{1}\bar{1}0\rangle$ parallel to ED oriented grains (designated as $\langle 10\bar{1}0\rangle$ grains and $\langle 2\bar{1}\bar{1}0\rangle$ grains, respectively hereafter) appear (Figures 3e,3f).

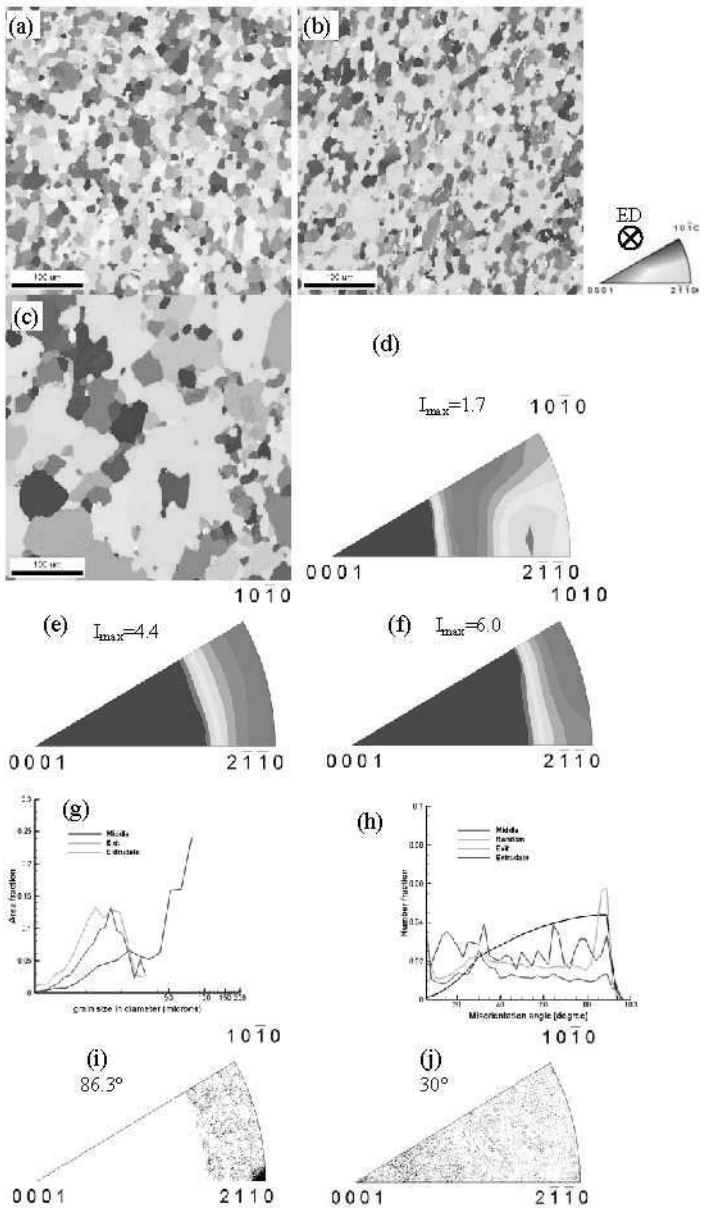

Figure 3: Microstructure and texture in different representative positions of the AM30 extruded at 450 °C and a ram speed of 10 mm/min. EBSD inverse pole figure (IPF) maps: (a) Middle; (b) Exit; and (c) Extrudate. The inverse pole figure of the extrusion direction (ED) in representative positions: (d) Middle; (e) Exit; and (f) Extrudate. (g) Grain size distribution; and (h) misorientation distribution and rotation axis/angle pair distribution at 86.3±2.5° (i) and 30±2.5° (j) in the Exit position. All these results are based on EBSD results in Figures 3(a)-(c). The color triangle represents the extrusion direction (ED).

Similar to 5 mm/min, grain dramatically grows in the Extrudate position as well (Figure 3g). The misorientation distribution and the rotation axis/angle pairs show that profuse twinning occurs at the Exit position. But twinning weakens in the Extrudate outside the die (Figure 3h). Twinning can be verified by the 86.3°<$1\bar{2}10$> orientation relationship which is the characteristic of $\{10\bar{1}2\}\langle 10\bar{1}\bar{1}\rangle$ twin boundary. Note that a misorientation peak

appears at around 30°, and a visible preferred rotation axis clustering at <0001> in the Exit position of the AM30 (Figures 3h,3j).

After extrusion, there is an evident transition area where some grains quickly grow at the expense of other grains. Figure 4 shows a typical transition area that includes both big grains and small grains at the ram speed 20 mm/min. In this case, two main texture components of $\langle 10\bar{1}0\rangle$ and $\langle 2\bar{1}\bar{1}0\rangle$ can be seen (Figures 4b,4c). Furthermore, $\langle 2\bar{1}\bar{1}0\rangle$ grain seems to grow preferentially over other orientations, e.g. the $\langle 10\bar{1}0\rangle$ grain. Grain size distribution shows a bimodal (Figure 4d). Misorientation distribution shows a high density of low angle grain boundaries (<6°), and a 30° and a 90° peak (Figure 4e). The misorientation and rotation axis/angle pair distribution show that $\{10\bar{1}2\}$ twins still exist in the Extrudate of the AM30 extruded at 450 °C and a ram speed of 20 mm/min (Figures 4e,4f). The misorienation 30° peak and the rotation axis/angle <u v w>δ° pair imply that <0001> 30° orientation relations may play roles on texture evolution (Figures 4e,4g).

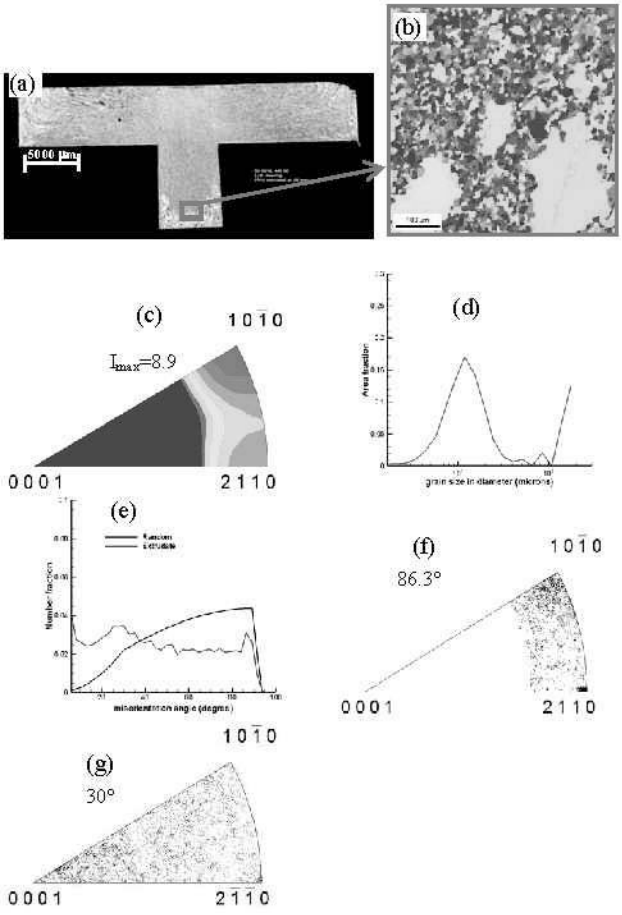

Figure 4: The microstructure and texture in the Extrudate position of the AM30 extruded at 450 °C and ram speed of 20 mm/min. (a) the microstructure of the Extrudate; (b) EBSD inverse pole figure map of the transition area from small grains to big grains; (c) inverse pole figure of ED; (d) grain size distribution; and (e) misorientation distribution and rotation axis/angle pair distribution at 86.3±2.5° (f) and 30±2.5° (g).

As ram speed increases to 30 mm/min, the Middle position texture appears different from the Exit position texture (Figures 5a-d). But grains grow not as much (Figure 5e). Misorienation distribution in the Middle looks similar to that in the Exit position. A high peak of low angle boundaries exists in the Middle and the Exit position. Strikingly, few twins are seen at the ram speed 30 mm/min according to misorientation and rotation axis/angle pair distribution (Figures 5f,5g). Similar to the case of ram speed of 10 and 20 mm/min, <0001>30° orientation relationship seems to play roles in microstructure and texture evolution during extrusion (Figures 5f,5h).

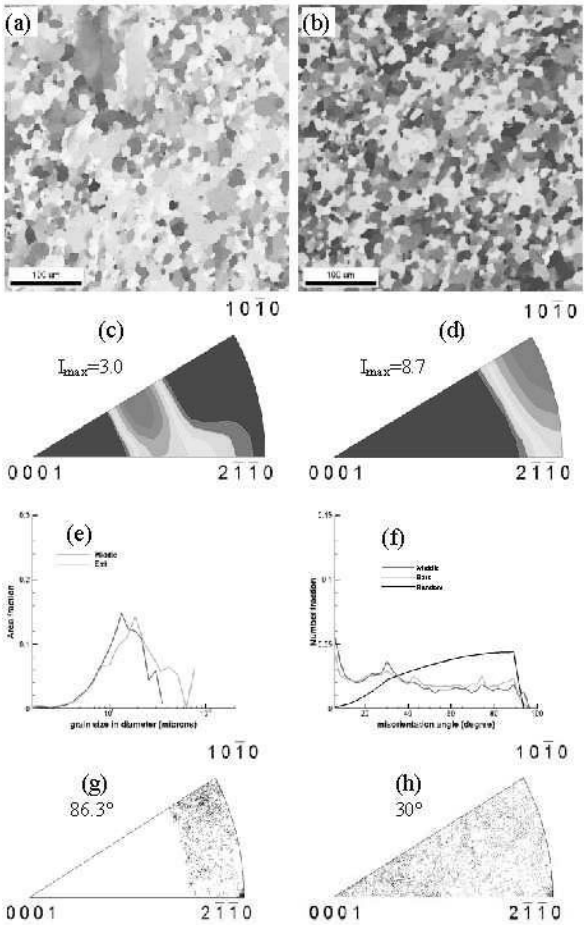

Figure 5: Microstructure and texture in the representative positions of the AM30 extruded at 450 °C and ram speed of 30 mm/min. EBSD inverse pole figure (IPF) maps in the representative positions: (a) Middle; (b) Exit; inverse pole figure of ED in the (c) Middle position, and (d) Exit position. (e) Grain size distribution; (f) misorientation distribution and rotation axis/angle pair distribution at 86.3±2.5° (g) and 30±2.5° (h) in the Exit position.

At ram speed of 50 mm/min, texture in the Middle position differs from those at ram speed of 10 mm/min and 30 mm/min (Figures 3d,5c,6d). But the texture in the Exit is similar at ram speeds of 10, 30, and 50 mm/min. A marked rotation tendency from $\langle 10\bar{1}0\rangle$ to $\langle 2\bar{1}\bar{1}0\rangle$ can be seen during extrusion at ram speed of 50 mm/min (Figures 6d-f). In the Extrudate position of the AM30, abnormal grain growth can be observed where $\langle 2\bar{1}\bar{1}0\rangle$ grains rapidly grow at the expense of other oriented grains (Figures 6c,6g). Misorientation and rotation axis/angle pair show that almost no $\{10\bar{1}2\}$ twinning activates during extrusion at the ram speed 50 mm/min. The <0001>30° orientation relation again be verified based on the misorienatation and rotation axis/angle distribution (Figures 6h,6j).

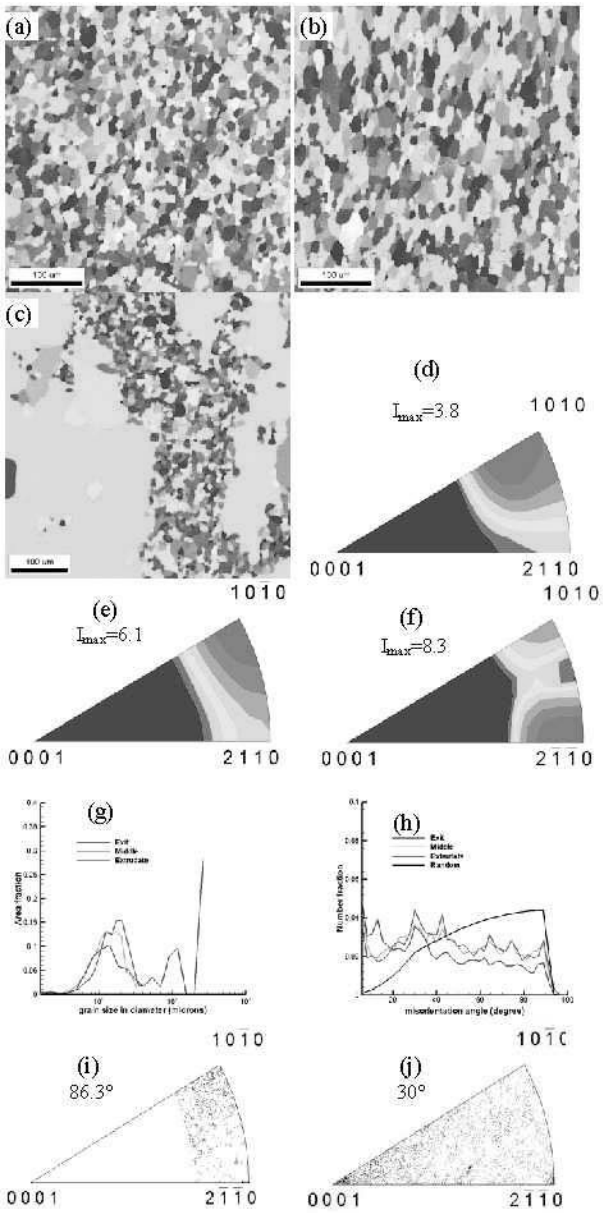

Figure 6: Microstructure and texture in representative positions of the AM30 extruded at 450 °C and ram speed of 50 mm/min. EBSD inverse pole figure (IPF) maps in the representative positions: (a) Middle; (b) Exit; (c) Extudate. The ED inverse pole figure at different positions: (d) Middle, (e) Exit; and (f) Extrudate. (g) Grain size distribution, and (h) misorientation distribution and rotation axis/angle pair distribution at 86.3±2.5° (i) and 30±2.5° (j) in the Extrudate position.

Discussion

During extrusion at high temperature of 450 °C, not only common deformation modes such as basal slip {0001}< $11\bar{2}0$ > and extension twinning $\{10\bar{1}2\}\langle 10\bar{1}\bar{1}\rangle$ will be activated, but also non-basal slips, including prismatic $\{10\bar{1}0\}<11\bar{2}0>$ slip and <*c*+*a*> pyramidal slips may also be activated . Meanwhile, DRX occurs and causes softening.

Extension $\{10\bar{1}2\}\langle 10\bar{1}\bar{1}\rangle$ twinning is predominant in Mg alloys; contraction twinning $\{10\bar{1}1\}\langle 10\bar{1}\bar{2}\rangle$ and double twinning $\{10\bar{1}1\}-\{10\bar{1}2\}$ are also often observed in Mg alloy near fracture [6,7]. Extension $\{10\bar{1}2\}\langle 10\bar{1}\bar{1}\rangle$ twins were observed in Mg alloys at 450 °C during extrusion and uniaxial compression [4,5]. In this study, $\{10\bar{1}2\}$ twinning is still activated at the ram speed of 10 mm/min (Figures 3h,3i). However, the $\{10\bar{1}2\}$ twinning subsides when the ram speed increases to 30 mm/min (Figures 5f,5g), and it is almost suppressed at the high ram speed 50 mm/min (Figures 6h,6i). Obviously, the $\{10\bar{1}2\}$ twinning behavior at 450 °C during extrusion differs from room temperature twinning. It is widely accepted that twinning is favored at low temperature and high strain rate [8,9]. However this former thought related to twinning may be not always the case. The critical resolved shear stress (CRSS) of slip is sensitive to temperature and strain rate [8]. This explains why texture is different in the same position of the Middle at different ram speeds (Figures 3d,5c,6d). However, twinning is considered athermal and the CRSS of twinning should be insensitive to temperature and strain rate [10]. At low temperatures, twinning easily initiates and accommodates plastic strain due to very limited number of easy slip systems [9]. However at high temperature, non-basal slips become more active because their CRSSs dramatically decrease [11].Thus slips and twinning compete to accommodate plastic strain at high temperature deformation at low strain rate. On the other hand, dislocation rearrangement and elimination, subgrain formation and growth induce strong recovery at high temperature in Mg [12]. Thus the matrix dislocation density may vary at different strain rates. The defect type and density within matrix may strongly affect the twin nucleation and growth. For example, in some bcc metals, twinning is totally suppressed by prestraining at high temperature [9]. Profuse twinning activated in AZ91 Mg alloy compressed at 300 °C at low strain rate of 0.05 s^{-1}, 0.1 s^{-1}, and 0.5 s^{-1}, but almost no twinning was found at high strain rate of 1 s^{-1} [13]. Thus twinning is hindered at high ram speed extrusion, e.g. 50 mm/min (high strain rate), but twinning is still activated at low speed extrusion (Figures 3h,3i). However, if strain rate is high enough that most slips are hard to activate, twinning could dominate deformation again. This interesting issue needs further study to clarify the underlying mechanism.

During extrusion, the original grains in the Middle position begin to deform and recrystallization occurs through grain boundary "bulging" and/or subgrain rotation inside matrix grain [12]. Thus the Middle position grain is finer than the original grain (Figures 2-6). Some grains coarsen in the Exit position due to grain growth via DRX. The driving force of DRX is the dislocation density difference across neighboring grains, and the grains grow via grain boundary migration. That means that the stable or "hard" oriented grains consume the unstable or "soft" oriented grains because the former has less dislocation density than the latter. In other words, the DRX texture of extruded AM30 exhibits a similar deformation texture without DRX. In extrusion, grains inside the die experience two main stresses: a compression stress along the radial direction (RaD) of the die and a tension stress along the extrusion direction (ED). The compression stress will force the *c*-axis of the grains parallel to compression axis due to the dominant basal slip, while the tension stress will force the $\langle 2\bar{1}\bar{1}0\rangle$ or $\langle 10\bar{1}0\rangle$ parallel to tensile axis because two prismatic slip systems have the same Schmid factor [14]. Thus during extrusion, only grains with the <0001> parallel to RaD and $\langle 2\bar{1}\bar{1}0\rangle$ or $\langle 10\bar{1}0\rangle$ parallel to ED are the stable grains.

Accordingly, grains in these orientations will survive and develop during extrusion. While other oriented grains will be consumed sooner or later by the stable grains. This explains why $\langle 2\bar{1}\bar{1}0\rangle$ grains or $\langle 10\bar{1}0\rangle$ grains mainly exist in the Exit position at all ram speeds extrusions (Figures 3-6). Due to activity of the prismatic slip, the rotation axis is <0001> and the rotation angle is 30° between $\langle 2\bar{1}\bar{1}0\rangle$ and $\langle 10\bar{1}0\rangle$. This is the reason the rotation axis/angle of <0001>30° exists at all ram speeds of the extrusions of AM30 at 450 °C.

When the AM30 exits the die, the $\langle 2\bar{1}\bar{1}0\rangle$ grains and $\langle 10\bar{1}0\rangle$ grains are the stable grains that have lower dislocation density due to the prismatic slip. Thus, the $\langle 10\bar{1}0\rangle$ and $\langle 2\bar{1}\bar{1}0\rangle$ grains grow at the expense of other oriented grains (Figure 3c). However, at high speed extrusions, more dislocations are reserved within the deformed grains due to anterior uncompleted DRX. Thus SRX well develops at rapid ram speed extrusion and abnormal grain growth is seen (Figures 4b,6c). Based on Figures 4b and 6c, some $\langle 2\bar{1}\bar{1}0\rangle$ grains abnormally grow by consuming other grains. It seems that at high ram speed extrusion, $\langle 2\bar{1}\bar{1}0\rangle$ grains are more stable than <10-10> grains. The transition from $\langle 10\bar{1}0\rangle$ to $\langle 2\bar{1}\bar{1}0\rangle$ was also reported in an extruded AZ31 Mg alloy during annealing at high temperature [15]. The reason was ascribed to the lower internal misorientation (less defects) in the $\langle 10\bar{1}0\rangle$ grains than other small grains. If this is the case, some $\langle 2\bar{1}\bar{1}0\rangle$ grains happen to form a domain that quickly involves a big grain via SRX. The big $\langle 2\bar{1}\bar{1}0\rangle$ grain rapidly grows and only large $\langle 2\bar{1}\bar{1}0\rangle$ grains dominate the final microstructure and texture in the extrudate (Figures 4b,6c).

Conclusions

A commercial AM30 Mg alloy was extruded at 450 °C and various ram speeds of 5, 10, 20, 30, and 50 mm/min in a lab-scale flat die. Microstructure and texture evolution during extrusion were examined by EBSD in different representative positions. Some conclusions can be drawn based on experimental results and analysis.

1) Deformation and DRX simultaneously occurred during extrusion inside the flat die. SRX started in the AM30 after it exited the die. The deformation, dynamic and static recrystallization dominate the final structure and texture of the extrudate.

2) $\{10\bar{1}2\}\langle 10\bar{1}\bar{1}\rangle$ extension twinning initiated at 450 °C during extrusion. Profuse twinning activated at low ram speed of 10 mm/min, but a few twins initiated at high ram speed of 50 mm/min. The reason could be that denser defects in matrix due to high speed extrusion hindered twinning nucleation and propagation.

3) Stress state of extrusion resulted in the two stable oriented grains: $\langle 2\bar{1}\bar{1}0\rangle \parallel$ ED and $\langle 10\bar{1}0\rangle \parallel$ ED grains. These two oriented grains grew at the expense of other oriented grains via grain boundary migration during DRX.

4) At high speed extrusion, the reserved defects within deformed grains served as driving force of SRX. The $\langle 2\bar{1}\bar{1}0\rangle$ grains had priority of abnormal growth at expense of other neighboring fine grains due to $\langle 2\bar{1}\bar{1}0\rangle$ grains being the most stable orientation during extrusion.

Acknowledgements

The authors are grateful to the financial support from the Department of Energy, Contract No. DE-FC-26-06NT42755, and the Center for Advanced Vehicular Systems (CAVS) at Mississippi State University.

References

1. A. Sadeghi and M. Pekguleryuz, "Recrystallization and texture evolution of Mg-3%-1%Zn-(0.4-0.8)%Sr alloys during extrusion", *Materials Science and Engineering A*, 528(2011) 1678-1685.
2. A.A. Luo, R.K. Mishra and A.K. Sachdev, "High-ductility magnesium-zinc-cerium extrusion alloys", *Scripta Materialia*, 64(2011) 410-413.
3. J.D. Robson, et al., "Effect of extrusion conditions on microstructure, texture, and yield asymmetry in Mg-6Y-7Gd-0.5 wt%Zr alloy", *Materials Science and Engineering A*, 528(2011) 7247-7256.
4. Q. Ma, et al., "Twinning-induced dynamic recrystallization in a magnesium alloy extruded at 450 °C", *Scripta Materialia*, 65(2011) 823-826.
5. Q. Ma, et al., "Strain rate dependence of twinning at 450 °C and its effect on microstructure of an extruded magnesium alloy", *Materials Science and Engineering A*, doi:10.1016/j.msea.2012.08.104, in press.
6. Q. Ma, et al., "Twinning effects in a rod-textured AM30 magnesium alloy", *International Journal of Plasticity*, 29(2012) 60-76.
7. Q. Ma, et al., "Twinning and double twinning upon compression of prismatic textures in an AM30 magnesium alloy", *Scripta Materialia*, 64(2011) 813-816.
8. M.A. Meyers, O. Vöhringer and V.A. Lubarda, "The onset of twinning in metals: A constitutive description", *Acta Materialia*, 49(2001) 4025-4039.
9. J.W. Christian and S. Mahajan, "Deformation twinning", *Progress in Materials Science*, 39(1995) 1-157.
10. A. Jain and S.R. Agnew, "Modeling the temperature dependent effect of twinning on the behavior of magnesium alloy AZ31B sheet", *Materials Science and Engineering*, A 462 (2007), 29-36.
11. A. Chapuis and J.H. Driver, "Temperature dependency of slip and twinning in plane strain compressed magnesium single crystals", *Acta Materialia*, 59 (2011), 1986-1994.
12. S.E. Ion, F.J. Humphreys and S.H. White, "Dynamic recrystallization and the development of microstructure during the high temperature deformation of magnesium", *Acta Metallurgica*, 30 (1982), 1909-1919.
13. L. Liu and H. Ding, "Study of the plastic flow behaviors of AZ91 magnesium alloy during thermomechanical process", *Journal of Alloys and Compounds*, 484(2009) 949-956.
14. T. Mayama, et al., "Crystal plasticity analysis of texture development in magnesium alloy during extrusion", *International Journal of Plasticity*, 27(2011) 1916-1935.
15. S. Yi, H.G. Brokmeier and D. Letzig, "Microstructural evolution during the annealing of an extruded AZ31 magnesium alloy", *Journal of Alloys and Compounds*, 506(2010) 364-371.